Journal of Magnetism and Magnetic Materials 329 (2013) 95–100

Contents lists available at SciVerse ScienceDirect

Journal of Magnetism and Magnetic Materials

journal homepage: www.elsevier.com/locate/jmmm

A complex magnetic structure of ultrathin Fe films on Rh (001) surfaces

Masaki Takada [a], Pedro Lana Gastelois [a,b], Marek Przybylski [a,c,*], Jürgen Kirschner [a,d]

[a] Max-Planck-Institut für Mikrostrukturphysik, Weinberg 2, 06120 Halle, Germany
[b] Serviço de Nanotecnologia, Centro de Desenvolvimento da Tecnologia Nuclear, 31270-901 BeloHorizonte, MG, Brazil
[c] Faculty of Physics and Applied Computer Science, AGH University of Science and Technology, 30-059 Kraków, Poland
[d] Naturwissenschaftliche Fakultät II, Martin-Luther-Universität Halle-Wittenberg, 06120 Halle, Germany

ARTICLE INFO

Article history:
Received 13 August 2012
Received in revised form
3 October 2012
Available online 13 October 2012

Keywords:
Magnetism of nanostructures
Magnetic measurements
Scanning tunneling microscopy
Surface structure

ABSTRACT

We conducted a structural and magnetic analysis of ultrathin Fe films on Rh (001) surfaces by using low electron energy diffraction (LEED), magneto-optical Kerr effects (MOKE) and spin-polarized scanning tunneling microscopy (SP-STM). The films in the investigated thickness range up to 6 monolayers (ML) are pseudomorphic to the Rh (001) substrate. While Fe films thinner than 3 ML grow layer-by-layer at room temperature (RT), Fe films thicker than 4 ML form islands. 1 ML Fe films do not show any hysteresis loops even at low temperature. Polar hysteresis loops for the 2 ML and 3 ML thick films appear at low temperatures. When 1 ML thick Fe films were studied by Cr- and Fe-coated W tips, a (2×3) and stripe structures were observed, respectively. The structures originate from a complex magnetic structure of 1 ML Fe. Based on the SP-STM results we propose a spin configuration model of a 1 ML Fe film.

1. Introduction

The magnetism of ultrathin Fe films strongly depends on their structure if grown on mismatching substrates. Fe films present particularly complex behaviors since they are variable with respect to their bcc or fcc crystallographic structure and therefore to their ferromagnetic (FM) or antiferromagnetic (AFM) ordering. Although the bulk γ-Fe phase, having an fcc crystallographic structure, occurs only at high temperatures and with no magnetic order, there are many theoretical and experimental reports discussing AFM order for thin Fe films of fcc structure stabilized by growing them on suitable substrates [1,2]. Additionally, many reports interpret low-moment ferromagnetism as a formation of the ferromagnetic fcc-like phase [1,2]. Moreover, unconventional spin states in ultrathin films, like the spin–spiral antiferromagnetic structure, have also been proposed if there is a competition between the FM and AFM exchange or the exchange coupling and the distinct magnetic anisotropies [3]. Considerable research has been done attempting to understand the complex structural and magnetic properties of epitaxial Fe thin-films and their subtle correlations.

One of the most important parameters that defines the different film magnetic phases is its lattice atomic volume, which can be explored by epitaxial growth on an appropriate substrate. One of the most interesting substrates is Rh. The atomic distance between the nearest neighbor Rh atoms is 0.269 nm. This value is located between those of ferromagnetic bcc Fe (0.287 nm) and antiferromagnetic fcc Fe (0.253 nm) if stabilized as small particles in a Cu matrix [4]. Fe films grown on Rh substrates could have more compressed or more expanded volume than bcc or fcc Fe, respectively. Thus, magnetic properties of Fe films grown on Rh surfaces are of interest.

Fe films on Rh surfaces have been studied by various experimental techniques, but these results contradict each other. Hwang et al. studied Fe films on Rh (001) by magneto-optical Kerr effect (MOKE) at room temperature (RT) and reported the suppression of the ferromagnetic order of Fe films thinner than 6 ML [5]. Hayashi et al. studied the magnetism of Fe films on Rh (001) by spin-resolved photoemission and X-ray magnetic circular dichroism (XMCD) experiments [6,7]. They observed different intensities for majority- and minority-spins for 3, 4 and 8 ML thick films. They measured a thickness dependence of $Fe^{3/2}_{2p}$ XMCD intensity at RT and at 97 K and also observed a ferromagnetic order in the Fe films thicker than 2 ML. Since there was no XMCD signal from Fe 1 ML films, they referred the 1 ML as a "magnetic dead layer".

The experimental studies mentioned above employed methods sensitive only to the presence or absence of ferromagnetic states. From previous experimental studies it is not clear whether zero net magnetization states, such as antiferromagnetism or a complex non-collinear state, exist in ultrathin Fe films. Theoretical calculations were carried out by two independent groups [8,9] and it was reported that 1 ML Fe films show a $c(2\times2)$ antiferromagnetic state with an in-plane magnetic anisotropy.

* Corresponding author at: Max-Planck-Institut für Mikrostrukturphysik, Weinberg 2, 06120 Halle, Germany. Tel.: +49 345 5582969; fax: +49 345 5511223.
E-mail address: mprzybyl@mpi-halle.de (M. Przybylski).

0304-8853/$ - see front matter © 2012 Elsevier B.V. All rights reserved.
http://dx.doi.org/10.1016/j.jmmm.2012.10.010

To reveal the local magnetic ordering, it is necessary to study Fe films with a method sensitive to atomic-scale magnetic structures. Spin-polarized scanning tunneling microscopy (SP-STM) is a suitable technique for studying complex magnetic structures, e.g, those showing zero magnetization (such as antiferromagnetic and non-collinear complex structures) with atomic resolution [3,10–12]. We studied the structural and magnetic properties of Fe films grown on Rh (001) surfaces with low electron energy diffraction (LEED), scanning tunneling microscopy (STM), spin-polarized STM (SP-STM), and MOKE measurements.

2. Experiments

A single crystal of Rh (001) was cleaned by Ar^+ sputtering and annealing at $T\sim900$ K. Fe films were deposited at room temperature from an electron beam deposition source. The structure of the Fe films was studied using LEED and STM. The magnetic properties of the Fe films were studied by SP-STM and MOKE. STM, SP-STM, and MOKE measurements were carried out mainly at 5 K. Wedge-shaped Fe films were fabricated for LEED and MOKE measurements. Our SP-STM experiments were performed using Cr-coated W (Cr/W) tips and Fe-coated W (Fe/W) tips which are claimed to be sensitive to the magnetization perpendicular and parallel to the sample plane [3,13–15], respectively. A W tip was flashed at a temperature above 2000 K. Cr and Fe films with a thickness of approximately 30 ML and 4 ML, respectively, were deposited onto the W tip at room temperature. SP-STM measurements were performed in the constant current mode [16].

3. Results

3.1. LEED and STM studies of Fe Films

The structure of Fe films grown on Rh (001) at RT was studied by LEED and STM. Fig. 1 shows LEED pattern of Fe films on Rh (001) surfaces measured at room temperature. LEED showed a (1×1) pattern for an Fe thickness between 1 ML and 6 ML. The spots were sharp and intense up to 3 ML. As the coverage was increased exceeding 4 ML, the spots became diffuse with an increase in the background signal. Begley et al., and Esawa et al., studied Fe films grown on Rh (001) surfaces with LEED up to a thickness of 5 ML and 9 ML, respectively [17,18]. Both observed the same (1×1) pattern as we observed. Begley et al. notably reported that the spots became blunt and the background signal increased as the thickness of Fe increased. Our results are in agreement with these previous LEED studies.

Fig. 2 displays STM images of different thicknesses of Fe films grown on Rh (001). In the thickness range up to 3 ML, the next layer does not start to grow unless the previous one is incomplete.

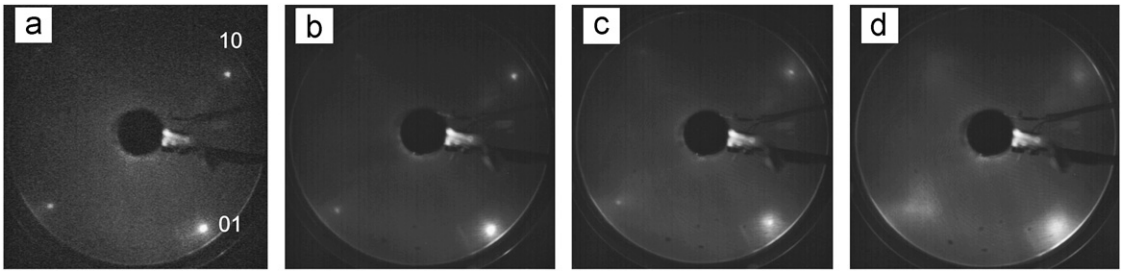

Fig. 1. LEED patterns of Fe films on Rh (001) surfaces. The thicknesses are (a) 1 ML, (b) 3 ML, (c) 4 ML and (d) 6 ML. The patterns were taken at room temperature for the electron energy of 37 eV.

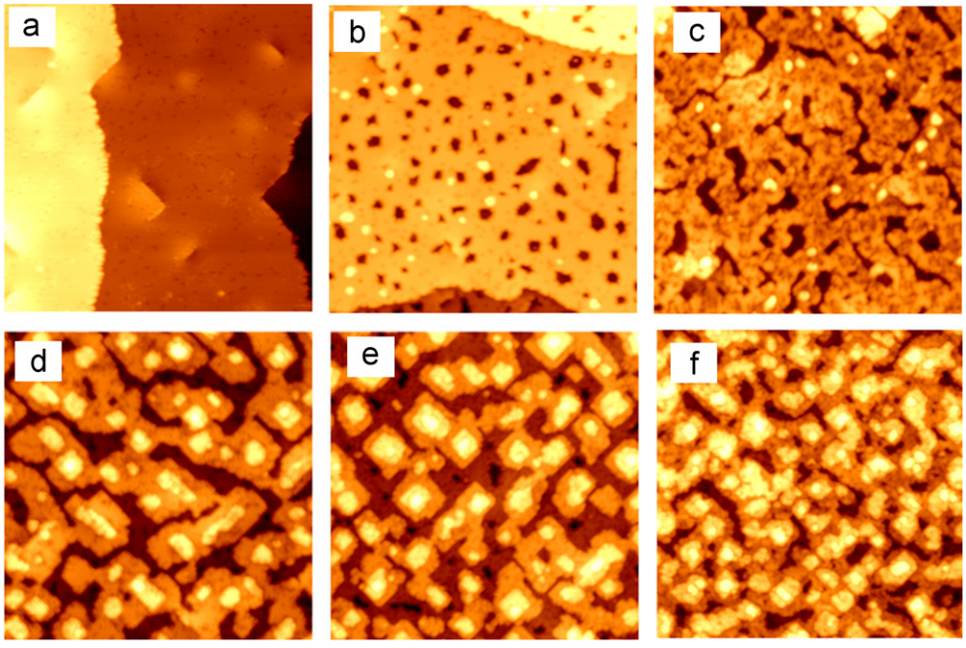

Fig. 2. STM images of bare Rh (001) surface(a) and Fe films of different thicknesses (b–f). The thicknesses are (b) 0.9 ML, (c) 1.9 ML, (d) 2.9 ML, (e) 3.9 ML and (f) 5.5 ML. The scan area for all images is 50×50 nm. All images were obtained with a W tip.

Thus one can conclude that the pseudomorphic Fe films grow layer-by-layer up to 3 ML. In Fig. 2(d), showing the STM image of 2.9 ML of Fe on Rh (001), the third and fourth layers cover ~80% and ~10% of the crystal surface, respectively. In Fig. 2(e) and (f), it is seen that the next layer clearly starts to grow before the previous layer covers the whole surface completely. These results indicate that the films thicker than 3 ML exhibit a 3-dimensional island growth, i.e., the transition from layer-by-layer to the island growth occurs at the thickness of 3 ML.

3.2. MOKE measurements of Fe Films

To investigate the magnetism of Fe films, MOKE measurements were carried out at 5 K. Fig. 3 shows the results. Fig. 3(a) shows polar Kerr ellipticity of Fe films (for the thickness range of 2.0, 2.5, 3.5, and 4.5 ML) versus an external magnetic field. Hysteresis polar square loops were measured up to a thickness of 3.5 ML. Fig. 3(b) shows longitudinal Kerr ellipticity for Fe films of thicknesses of 3.5, 4.0 and 4.5 ML. Clear hysteresis loops appear for films thicker than 4.0 ML measured in longitudinal geometry. At RT, MOKE measurements show that Fe films thicker than 4 ML are ferromagnetic. While MOKE measurements at RT for Fe films thinner than 4 ML show no hysteresis loops in both longitudinal and polar geometry, ferromagnetic states for films thinner than 4 ML appear only at temperatures lower than RT.

Thickness dependence of polar and longitudinal Kerr ellipticity in remanence for Fe films on Rh (001) surfaces measured at 5 K is shown in Fig. 3(c). For Fe films thicker than 2 ML, polar Kerr ellipticity increases with increasing film thickness. However, the polar Kerr ellipticity signal decreases abruptly to zero at a thickness of 4 ML. Around the same thickness, the longitudinal Kerr ellipticity signal starts to increase with increasing thickness. In the longitudinal MOKE, there are no loops observed for Fe films thinner than 4 ML. The MOKE results indicate that Fe films thicker than 2 ML are ferromagnetic and exhibit clear magnetic anisotropy that depends on the film thickness. The easy magnetization axis of Fe films thinner and thicker than 4 ML is oriented out-of-plane and in-plane, respectively. Since neither polar nor longitudinal Kerr ellipticity of Fe films thinner than 2 ML show any hysteresis loops, 1 ML Fe films are considered to have a complex magnetic structure, which exhibits zero net magnetization. In part, such structure can be due to spin polarization of the Rh substrate [19].

3.3. SP-STM observation of Fe 1 ML films with a Cr-coated W tip

SP-STM was employed for identifying the magnetic structure of 1 ML Fe films. Fig. 4(a) shows an SP-STM image of a 0.9 ML Fe film observed with a Cr/W tip. In Fig. 4(a), periodic structures along the [110] and [$\bar{1}$10] directions appear in the regions indicated by white rectangles. Fig. 4(b) is an enlarged image of the lower right region of Fig. 4(a). The periodic structure with a unit cell size, indicated by a black-dotted rectangle, is clearly recognizable. For comparison, an STM image of an 1 ML Fe region observed with a non-magnetic bare W tip is shown in Fig. 4(c). The image size is the same as that of Fig. 4(c) indicated in Fig. 4(b) by a white rectangle. These structures, as probed with a Cr/W tip and a bare W tip, are completely different. When the 1 ML Fe is imaged with a W tip, only a (1×1) structure appears. This indicates that the (1×1) structure corresponds to the topological/crystallographic arrangement of the Fe atoms. There was no other structure observed that is related to an intermixing or alloying. Thus, we concluded that the (2×3) structure probed with a Cr/W tip (and shown in Fig. 4(b)) is of spin origin and originates from the spin configuration of 1 ML Fe films.

The line profiles along the [110] direction of the (2×3) structure are shown in Fig. 4(d). For easier comparison, the red line is shifted laterally along [$\bar{1}$10] by half the symmetry period with respect to the blue line. Since a Cr/W tip is claimed to be sensitive to the out-of-plane component of the surface spin configuration [13,14], the periodic oscillation in Fig. 4(d) represents the oscillation of the out-of-plane component of the spin of each Fe atom. As shown by a dashed line in Fig. 4(d), the valleys of the red line are of depths similar in magnitude to the peaks of the blue line. This indicates that the out-of-plane valleys along the red line are of the same magnitude as those of the peaks along the blue line. A possible spin configuration along the red and blue lines of Fig. 4(b) is shown schematically in Fig. 4(d) with red and blue arrows, respectively.

3.4. SP-STM observation of Fe 1 ML films with an Fe-coated W tip

1 ML Fe films have also been studied by using an Fe/W tip claimed to be sensitive to the in-plane magnetization components [3,15]. The resulting images show different patterns from those obtained with a Cr/W tip. Fig. 5(a) shows an SP-STM image of Fe 1 ML observed with an Fe/W tip. A stripe structure with a period of ~0.9 nm is recognized along the [150] or [510] directions. This pattern indicates that the Fe/W tip is sensitive to the different spin components in comparison to the Cr-covered W tip. Each stripe tends to consist of oval-shaped dots arranged in a line. The stripe structure observed with the Fe/W tip is less ordered than the (2×3) structure observed by a Cr/W tip. This is because the area showing the (2×3) structure is typically not larger than 4×4 nm, which corresponds only to about 4 times the period of the stripe structure. This is not sufficient to show the stripe structure on larger areas.

Fig. 5(b) and (c) shows SP-STM images of the same area observed by an Fe/W tip before and after the magnetization of the tip was reversed. The magnetization reversal of the tip happened by chance.

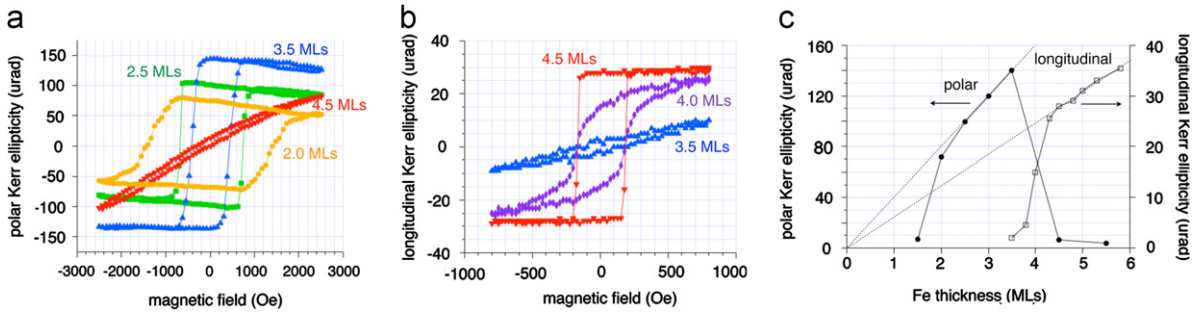

Fig. 3. (a) Polar Kerr ellipticity loops of Fe films grown at RT on an Rh (001) surface. The film thickness is 2.0 (orange), 2.5 (green), 3.5 (blue) and 4.5 ML (red). (b) Longitudinal Kerr ellipticity loops of Fe films grown on Rh (001) at RT. The thickness is 3.5 (blue), 4.0 (purple) and 4.5 (red). (c) Thickness dependence of polar and longitudinal remanent Kerr ellipticity for Fe/Rh (001). Filled circles and empty squares represent polar and longitudinal Kerr effects, respectively. All of the MOKE measurements were carried out at 5 K.

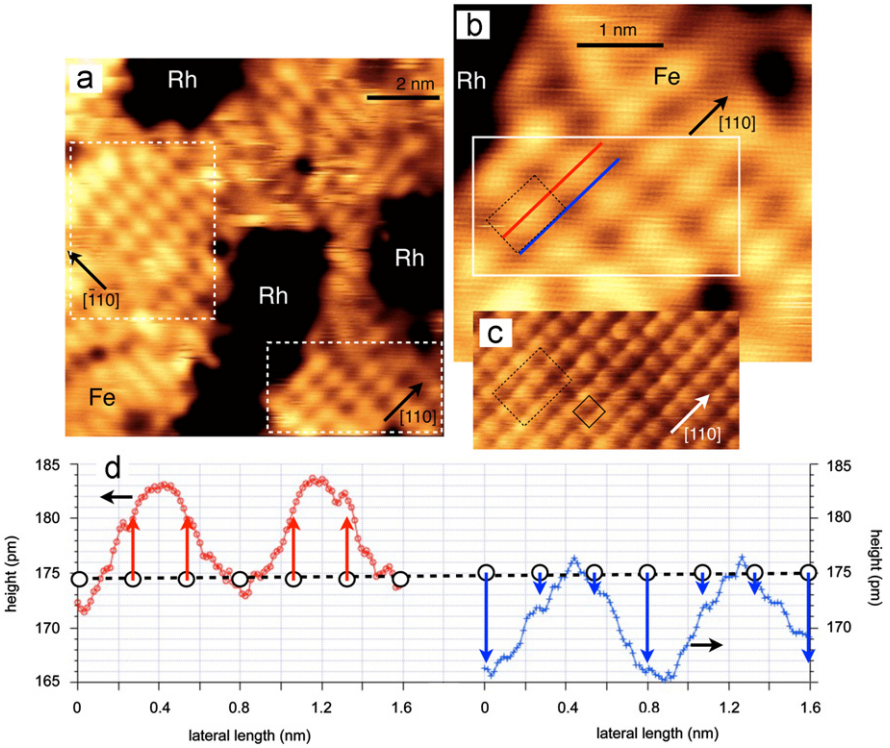

Fig. 4. (a) SP-STM images of 0.9 ML Fe on Rh (001) observed with a Cr/W tip. The thickness of the Cr covering the W tip is approximately 30 ML. The scan area of (a) is 10×10 nm. The sample bias voltage and the tunneling current are +40 mV and 5 nA, respectively. (b) Enlarged SP-STM image of the (2×3) structure of 1 ML Fe films. The unit cell is represented by a dashed rectangle. For comparison, an atom-resolved STM image of an Fe 1 ML region probed with a bare W tip is shown in (c). The same image size as (c) is indicated in (b) by a white rectangle. In (c), the (1×1) unit cell and the (2×3) cell are indicated by a square and by dotted rectangles, respectively. (d) Line profiles along the red and blue lines in (b). The red circles and blue crosses represent the profiles along the red and blue lines, respectively. The profiles are shifted in the lateral direction for easier comparison. The dashed line is drawn to indicate that the valleys of the red line are of the same magnitude as the peaks of the blue line. In (d), a schematic model of the out-of-plane spin components is shown with circles and arrows. The circles represent the positions of the Fe atoms. The arrows correspond to the out-of-plane spin components.

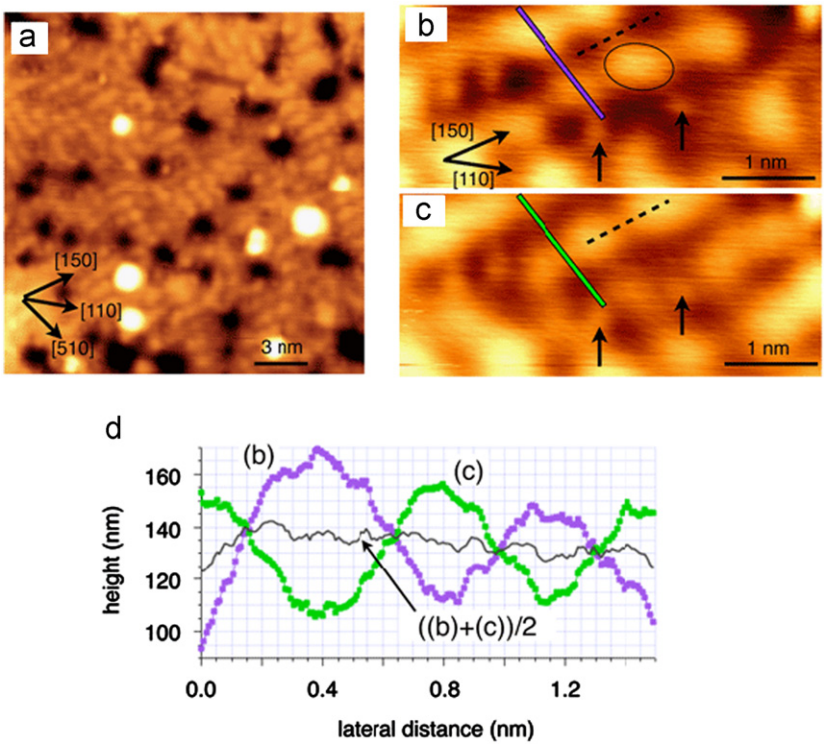

Fig. 5. (a) SP-STM images of Fe 0.9 ML on Rh (001) observed with an Fe/W tip. The thickness of the Fe films covering the W tip is 4 ML. The scan area is 20×20 nm. The sample bias voltage and the tunneling current are +30 mV and 5 nA, respectively. (b) and (c) are SP-STM images of the same area of the 1 ML Fe film probed with a magnetization-reversed Fe/W tip. The scan area of both images is 2×4.5 nm. The arrows indicate the positions of the impurities. The dotted lines indicate the position at which the contrast is inverted. An oval-shaped structure is indicated by an oval in (b). The cross-section along the purple and green bars in (b) and (c) are shown in (d), respectively. The black line in (d) is half of the sum of the red (b) and blue (c) lines.

An oval-shaped dot structure is indicated by an oval in Fig. 5(b). Five oval-shaped dots are linearly distributed along the [150] direction. The size of each oval dot is similar to the size of the (2×3) unit cell observed by a Cr/W tip. In Fig. 5(b) and (c), the positions of the impurities, indicated by arrows, are not changed by the reversal of the tip magnetization. The stripe structure runs along the direction of the black dashed lines, but the contrast is inverted at every atom. The line profiles along the purple and green bars in Fig. 5(b) and (c) are shown in Fig. 5(d). The contrast inversion is very obvious here. The Fe/W tip shows the different stripe pattern from the (2×3) pattern observed with the Cr/W tip, indicating that the Fe/W tip is sensitive to the different spin components. Thus, in extension to the previous studies [3,15], one can conclude that the Fe/W tip successfully detects the in-plane surface magnetization component. The stripe structure observed in this study reflects the in-plane component of the spin configuration for 1 ML-thick Fe films.

4. Discussion

From MOKE measurements, Fe films thicker than 2 ML on Rh (001) surfaces are found to be ferromagnetic. The magnetic anisotropy of Fe films on Rh (001) surfaces is thickness-dependent. The easy magnetization axis of 2 ML and 3 ML thick Fe films is oriented out-of-plane. However, the easy magnetization axis of Fe films thicker than 4 ML is oriented in the sample plane.

MOKE measurements of 1 ML Fe films show no hysteresis loop in both polar and longitudinal geometries even at low temperature (5 K), which indicates that 1 ML Fe films are not ferromagnetic, but are expected to exhibit a magnetic configuration with a zero net magnetization. It is therefore necessary to apply an experimental method sensitive to the local spin configuration. Thus, SP-STM measurements were carried out for 1 ML Fe films.

SP-STM with a Cr/W and Fe/W tip exhibit (2×3) and stripe structures, respectively. There is no indication of the $c(2 \times 2)$ antiferromagnetic spin configuration predicted by theoretical calculations [8,9]. From the SP-STM measurements, using Cr/W and Fe/W tips, 1 ML Fe film is considered to exhibit a complicated non-collinear spin configuration with zero net magnetization. A possible model of the spin arrangement of 1 ML Fe film is proposed in Fig. 6. The configuration of the out-of-plane (Fig. 6(a)) and in-plane (Fig. 6(b)) spin components are deduced from the (2×3) structure detected with a Cr/W tip (Fig. 4), and the stripe structure detected with an Fe/W tip (Fig. 5), respectively. In Fig. 6(a), both up- and down-spin components are aligned along the [110] direction as deduced from Fig. 4(d). Here, all out-of-plane components balance each other within a unit cell. Fig. 6(b) is a model of the in-plane components deduced from the SP-STM results obtained with an Fe/W tip. In Fig. 6(b), the magnetic anisotropy of in-plane components is assumed to be along the $[\bar{1}10]$ direction. The stripe structure appearing in Fig. 5 is indicated by blue lines along the [150] direction. The (2×3) unit cells, indicated by thick rectangles, are aligned along the [150] direction. This alignment of the (2×3) unit cells is equivalent to that of the oval-shaped dots as shown in Fig. 5(b). Fig. 6(c) is a 3-dimensional model of 1 ML Fe films derived from Fig. 6(a) and (b). The model in Fig. 6(c) is possibly one of the simplest models ever proposed. Fig. 6(d) shows the same model as Fig. 6(c) but viewed along the [150] direction. Helical spin structures are recognized along the [150] direction as indicated by the black arrows. The relative size of the in-plane and out-of-plane magnetic components between the results obtained with a Cr/W and an Fe/W tip cannot be determined from the present

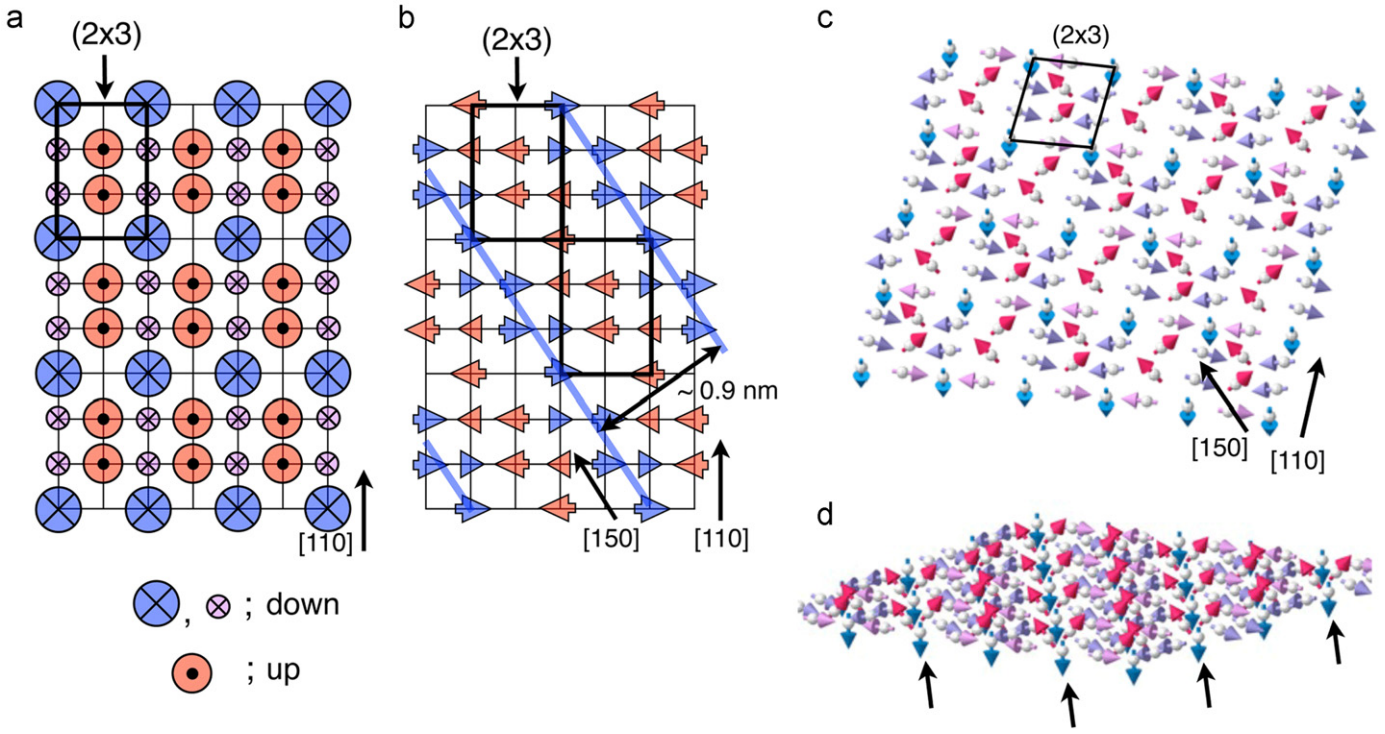

Fig. 6. Proposed model of the spin configuration of 1 ML Fe on a Rh (001) surface. (a) Configuration of out-of-plane spin components. (b) Configuration of in-plane spin components. The size of the circle and the length of the arrows in (a) and (b) correspond to the relative size of the out-of-plane and in-plane components, respectively. The grid shows the atomic arrangement. (c) 3-dimensional model of the spin configuration. The gray balls represent Fe atoms. The arrows indicate the spin directions. The blue arrows represent spin components which are completely down. Red arrows indicate spins with a polar angle of 41°. The purple arrows indicate spin configurations which have relatively large in-plane components (polar angle is 76° or 90°). In (d), the same 3-dimensional model as (c) is viewed along [150] direction. The black arrows indicate the direction along which the helical spin structures are recognized.

study. To determine an accurate model, further SP-STM analysis under an external magnetic field would be necessary.

There are no theoretical studies available which predict a complex magnetic structure for 1 ML Fe on Rh (001) surfaces. However, a complex magnetic structure is theoretically predicted for 1 ML Fe on an Ir (001) surface which has, as Rh (001), an fcc crystallographic structure and a similar lattice constant [20,21]. Here, based on the theoretical predictions for 1 ML Fe on Ir (001), we discuss a possible origin of the complex spin configuration as we experimentally observe for 1 ML Fe on Rh(0 0 1). There can be three possible origins causing the spin configuration complex: (1) 3d–4d hybridization between Fe and Rh at the interface, (2) Dzyaloshinskii–Moriya interaction (DMI), and (3) multiple spin interaction such as biquadratic interaction.

Kudrnovský et al. [20] studied the effect of orbital hybridization between Fe and Ir on the magnetic structure of 1 ML Fe by systematically changing the interlayer distance between 1 ML Fe and the Ir (001) substrate. By decreasing the interlayer distance, a spin–spiral-like magnetic order can be induced. A similar tendency is expected for 1 ML Fe on Rh (001) as discussed in the same paper [20]. The hybridization between the 3d electrons of Fe and the 4d electrons of Rh can affect the magnetic order of 1 ML Fe. However, the predicted magnetic structure is rather simple if compared to the complex spin configuration obtained in our study. This can be due to the DMI and/or multiple spin interactions which are absent in the model [20]. Also, the previous theoretical calculations by Spišák and Hafner [8] and Al-Zubi et al. [9] do not allow the DMI nor the biquadratic interaction.

The DMI is a particularly important interaction which often results in a complex magnetic ordering. Deák et al. [21] calculated possible spin configurations for 1 ML Fe on Ir (001) surfaces by including the DMI, and thereby obtained a complex helical spin ordering. Also, the biquadratic spin interaction term was tested showing a different spin configuration, but of the same spatial modulation. Both predicted spin configurations [20,21] are different from the model deduced from our SP-STM observations. It is most likely that the complex magnetic configuration observed experimentally results from a competition between the exchange interaction caused by the orbital hybridization, the DMI, and the biquadratic spin interaction.

At the end we would like to stress that the spin configuration obtained from the SP-STM observation, resulting in zero net magnetization, remains in excellent agreement with the results of the MOKE measurements.

5. Conclusions

In summary, we studied structural and magnetic properties of Fe films grown on an Rh (001) surface. STM observations reveal that the transition from layer-by-layer to the island growth persists up to the 3 ML thickness. MOKE measurements revealed that Fe films thicker than 2 ML are ferromagnetic with the magnetic anisotropy being thickness-dependent. While Fe films with a thickness of 2 ML and 3 ML exhibit out-of-plane magnetization, those thicker than 4 ML show in-plane magnetization. From MOKE and SP-STM measurements, we found that 1 ML Fe films have a complex magnetic configuration with zero net magnetization. A spin configuration model of 1 ML Fe was proposed based on an SP-STM observation with a Cr/W and an Fe/W tip. This is in agreement with the zero Kerr signal measured for 1 ML of Fe on Rh (001) by MOKE. Detailed theoretical calculations of the spin configuration, which include orbital hybridization, DMI and quadratic spin interaction, should be applied to a 1 ML Fe/Rh (00 1) system. Then the origin of the complex spin configuration of 1 ML Fe/Rh (001), deduced from our SP-STM studies, could be analyzed.

References

[1] V.L. Moruzzi, P.M. Marcus, K. Schwarz, and P. Mohn, Physical Review B 34, 1784 (1986).
[2] D. Spišák, J. Hafner, Physical Review Letters 88 (2002) 056101.
[3] M. Bode, E.Y. Vedmedenko, K. von Bergmann, A. Kubetzka, P. Ferriani, S. Heinze, R. Wiesendanger, Nature Materials 5 (2006) 477.
[4] S.C. Abrahams, L. Guttman, J.S. Kasper, Physical Reviews 127 (1962) 2052.
[5] C. Hwang, A.K. Swan, S.C. Hong, Physical Review B 60 (1999) 14429.
[6] K. Hayashi, M. Sawada, A. Harasawa, A. Kimura, A. Kakizaki, Physical Review B 64 (2001) 054417.
[7] K. Hayashi, M. Sawada, H. Yamagami, A. Kimura, A. Kakizaki, Journal of the Physical Society of Japan 73 (2004) 2550.
[8] D. Spišák, J. Hafner, Physical Review B 73 (2006) 155428.
[9] A. Al-Zubi, G. Bihlmayer, S. Blügel, Physical Review B 83 (2011) 024407.
[10] C.L. Gao, U. Schlickum, W. Wulfhekel, J. Kirschner, Physical Review Letters 98 (2007) 107203.
[11] C.L. Gao, A. Ernst, A. Winkelmann, J. Henk, W. Wulfhekel, P. Bruno, J. Kirschner, Physical Review Letters 100 (2008) 237203.
[12] C.L. Gao, W. Wulfhekel, J. Kirschner, Physical Review Letters 101 (2008) 267205.
[13] A. Kubetzka, M. Bode, O. Pietzsch, R. Wiesendanger, Physical Review Letters 88 (2002) 057201.
[14] G. Rodary, S. Wedekind, H. Oka, D. Sander, J. Kirschner, Applied Physics Letters 95 (2009) 152513.
[15] K. von Bergmann, S. Heinze, M. Bode, E.Y. Vedmedenko, G. Bihlmayer, S. Blügel, R. Wiesendanger, Physical Review Letters 96 (2006) 167203.
[16] D. Wortmann, S. Heinze, Ph. Kurz, G. Bihlmayer, S. Blügel, Physical Review Letters 86 (2001) 4132.
[17] A.M. Begley, S.K. Kim, F. Jona, and P.M. Marcus, Physical Review B 48, 1786 (1993).
[18] C. Egawa, Y. Tezuka, S. Oki, Y. Murata, Surface Science 283 (1993) 338.
[19] A. Lehnert, S. Dennler, P. Blonski, S. Rusponi, M. Etzkorn, G. Moulas, P. Bencok, P. Gambardella, H. Brune, J. Hafner, Physical Review B 82 (2010) 094409.
[20] J. Kudrnovský, F. Máca, I. Turek, J. Redinger, Physical Review B 80 (2009) 064405.
[21] A. Deák, L. Szunyogh, B. Ujfalussy, Physical Review B 84 (2011) 224413.